A Visual Motion Detecting Module for Dragonfly-Controlled Robots

Thuy T. Pham and Charles M. Higgins

Abstract— **When imitating biological sensors, we have not completely understood the early processing of the input to reproduce artificially. Building hybrid systems with both artificial and real biological components is a promising solution. For example, when a dragonfly is used as a living sensor, the early processing of visual information is performed fully in the brain of the dragonfly. The only significant remaining tasks are recording and processing neural signals in software and/or hardware. Based on existing works which focused on recording neural signals, this paper proposes a software application of neural information processing to design a visual processing module for dragonfly hybrid bio-robots. After a neural signal is recorded in real-time, the action potentials can be detected and matched with predefined templates to detect when and which descending neurons fire. The output of the proposed system will be used to control other parts of the robot platform.**

I. INTRODUCTION

Biologically inspired systems have been designed with inspiration from biology and principles underlying the neural control in animals. For example, using models of insect eyes, Jeong et al. [1] have created artificial compound eyes with thousands of tiny lenses packed side by side. These eyes are expected to be used in camcorders for omnidirectional surveillance imaging. However, in simple applications of robotics (e.g., target tracking or collision avoidance), such artificial eyes may not be suitable for low-cost mobile neuromorphic systems. Moreover, to reproduce biological visual sensors better, we still need more efforts to make these eyes more comparable to those found in nature [2]. Additionally, the early processing of the visual information has not been understood completely. A hybrid bio-robotics approach provides a promising solution for low-cost mobile neuromorphic systems. Since 2005 the Higgins laboratory (University of Arizona) has been interfacing the living brains of moths to mobile robots. They designed prototype electrophysiological recording printed circuit boards (PCBs) [3] and a PCB that is capable of running in real time a software module for signal processing with four neural signal recording channels [4]. Melano used Ortiz's design in [3] to interface directionally-sensitive visual neurons and pleurodorsal steering muscles of the mesothorax with a robot [5].

With this robotic approach, we managed to create visual sensor inputs of a robot from dragonflies' descending neurons. The dragonfly has attracted our attention due to its excellent vision. Dragonflies have the largest compound eyes of any insect; each containing up to $30,000$ facets. An adult dragonfly can see in almost all directions at the same time. Sensory signals of dragonflies are transferred from the brain to thoracic ganglia through neurons called *descending interneurons*. There are eight large individual descending neurons that are very visual target-selective ("*TSDNs*") [6]. Their visual receptive field properties were analyzed well by Frye et al. [7]. From these properties of TSDNs, we detected and classified action potentials ("spikes") in electrophysiological signals. Then, we defined spike templates for these TSDNs to recognize which ones transmit which spikes. In this study, this process is called *spike sorting*. Spike detecting can be performed by threshold-based methods, energy-based methods, or template-based ones. To detect spikes in real time we need to use a simple algorithm. Though the threshold-based methods execute relatively simple computation, they are sensitive to noise and require a step of setting threshold levels [8]. The energy-based methods involve a nonlinear energy operator (NEO) to estimate the square of the instantaneous product of amplitude and frequency of a sufficiently sampled signal [9] while the template-based methods match spikes with filters. The latter one involves multiple convolutions, it should not be a candidate for real-time multichannel systems. From the review by Obeid et al. [8], we chose the NEO algorithm to detect spikes.

We built spike templates through two main steps: extracting spike features, and then classifying spikes by these features. Common spike feature extraction algorithms are based on principal component analysis [10] and the discrete wavelet transform (DWT) [11]. Current algorithms classify similar spikes by k-means clustering [12], Bayesian classification [13], and super paramagnetic clustering (SPC) [14]. Extraction algorithms have been reviewed recently while classification algorithms have been in need of a newer review since 1998. From a recent review [15] and other criteria of the system design (e.g. high accurate spike-feature extraction), we chose the DWT and SPC approaches for the proposed system. In summary, this paper proposes a design for a visual motion detecting module in dragonfly-controlled robots. Properties of the TSDNs are discussed first to provide a background for neural information interpretation, then a system architecture design is presented. We investigated the performance and provided finally concluding remarks.

II. TARGET SELECTIVITY PROPERTIES OF DRAGONFLY DESCENDING NEURONS

In the dragonfly, eight descending neurons in the ventral nerve cord control oriented flight responses to the image of target in the retina [6]. They are named according to the longitudinal tract through which these neurons pass in the prothoracic ganglion: DIT1, DIT2, and DIT3 for

Thuy T. Pham and Charles M. Higgins: Department of Electrical and Computer Engineering and Department of Neuroscience, University of Arizona, AZ USA 85716. phamt@ece.arizona.edu, higgins@neurobio.arizona.edu

978-1-4244-7929-0/14/$26.00

the dorsal intermediate tract; and MDT1, MDT2, MDT3, MDT4, and MDT5 for the median dorsal tract [7]. These interneurons have some similar characteristics. All of them descend from the brain and have very big axons. They all responded selectively to the movement of small target [6]. Five of the eight TSDNs have strong directional preferences: MDT1, MDT2, MDT4, MDT3, and DIT1. Frye et al. [7] identified the visual receptive field properties of these TSDNs by recording responses when moving a target in each of four orthogonal directions on a 90^ox90^o screen. Across the preparations, the location and the directional preference of the receptive fields remained constant, but the strength of the response and the size of the receptive field varied. We used these properties as a ground truth to detect a TSDN.

III. HARDWARE ARCHITECTURE DESIGN

We propose a real-time neural signal processing system with a combination of PCB-based hardware and FPGA-based software modules. The PCB-based provides analog signal recording and digital signal processing functions. To avoid interference between the different formats of signal processing (analog and digital) and a small-size requirement,we construct two separate PCBs. The analog PCB is designed with high-pass filters (HPFs), low-pass filters (LPFs) and notch filters to remove noise, electricity interference. We employed the PCB with configurable cut-off frequencies to configure a suitable setting for a particular recording condition. The digital PCB contains a soft-core processor and a memory subsystem. The soft-core processor is generated in a hardware description language and can be implemented by an FPGA device. We include external memories (SRAM and Flash) to support multi-channel processing tasks. Because of the mobility requirement and convenience for power saving, an automatic configuration ability of this FPGA device is preferred. To fit well into a small rack of a hybrid bio-robot, the PCBs should have small dimensions and consume little power supply. Fig. 1 captures our recently fabricated PCB.

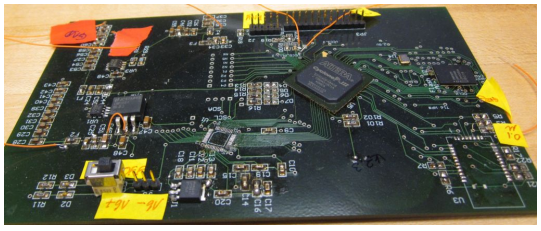

Fig. 1. Recently fabricated digital PCB version in the Higgins laboratory.

To control the robot platform and remotely monitor, beside headers for wire connection we embed a wireless transmitter station for Bluetooth connections. This station is chosen to have small space occupation, low power consuming, and high-speed transmission. In our design, it consumes as low power as 30 mA in the connecting mode (10 mA in the sniff mode) and can deliver up to $3Mbps$ for distances to $100m$.

IV. SOFTWARE ARCHITECTURE DESIGN

As the eight TSDNs contain the visual "sensing" signals from the brain when a dragonfly is seeing a moving target, we can use the visual receptive field properties to guide a robot platform. Thus, we need to detect when and which TSDN fires a spike from given recording signals. A time instant of firing can be found by applying a spike-detection algorithm, e.g. NEO in our case. To know which one of the eight TSDNs a spike belongs to, we use a template-matching method. Specifically, if a detected spike form matches very well (quantified by a high correlation coefficient) with a spike-template of a TSDN. Templates were pre-defined by classifying spikes from given special stimulus data sets. We built these templates with the DWT method for spike-feature extraction and the SPC method for spike clustering.

A. Selected Algorithms

NEO provides the instantaneous energy of the high pass filtered version of a signal. This feature makes NEO an ideal detector of transients [16]. DWT relies on the wavelet analysis technique to extract features of a spike. Basically, to find differences among spikes, DWT is based on the quantification of energy found in specific frequency bands at specific time locations. In the SPC clustering method, the ferromagnetic phase, the paramagnetic phase, and the super paramagnetic phase can be considered a classification of one single cluster, several tiny clusters, and a number of medium-size clusters, respectively. Using the recommended setting by Blatt et al. [17] (20 states, 11 nearest neighbors, and 500 iterations), the clustering process would mainly depend on the temperature parameter and is robust to small changes of other parameters. Once templates were built, we used correlation-based template matching method to know which one of the eight TSDNs a spike belongs to. The relevant neuron corresponds to the best-matched template, i.e., the one that has the highest correlation coefficient $r_{X,Y}$ with the spike (1). The highest $r_{X,Y}$ should also be higher than a level Cr that we expect the assignment is true (see Section V-B).

$$r_{X_i,Y_j} = \frac{\mathcal{C}\{X_i, Y_j\}}{\sigma_{X_i}\sigma_{Y_j}} \tag{1}$$

where r_{X_i,Y_j} is the correlation coefficient between the i^{th} spike of a spike set X and the j^{th} template of a template set Y. $\mathcal{C}\{X_i, Y_j\}$ is the covariance of X_i and Y_j. σ_{X_i} and σ_{Y_j} are the variances of X_i and Y_j, respectively.

B. Neural Signal Processing

To build spike-templates for the eight TSDNs we gave special visual stimuli then collected appropriate spike-form samples. These special visual stimuli are designed to strongly stimulate a particular TSDN according to given properties. For example, if a moving target starts from the bottom right corner of a stimulus screen with anterior orientation, there will be spikes that mostly come from the MDT2 neuron. After detecting all spikes in this stimulation case, we can cluster

TABLE I

VISUAL STIMULATION AND CORRESPONDING TEMPLATES.

Orientation	Starting at	Segment	Templates
Posterior	Bottom far right	Early	DIT3
Posterior	Bottom far right	Later	DIT1
Anterior	Bottom far right	Whole	MDT2
Dorsal	Top center	Whole	MDT1
Dorsal	Top left	Whole	MDT3
Ventral	Bottom right	Whole	MDT4

them to find the largest group of similar spike samples. The average spike form of this group is then considered a spike-template of MDT2. We built a total of six templates upon the specifications of visual stimulation arrangements (Table I) and names them after the respective TSDNs. Five templates are for all strongly directionally selective neurons (MDT1, MDT2, MDT3, MDT4, and DIT1). The sixth template is for DIT3, serving as an example of a neuron that is not strong directionally selective.

Though we have groups clustered automatically, we assess reasonable template information manually. Hence, the performance of the whole application depends not only on the special visual stimuli we set up, and on the rightness of the receptive field properties but also on the experience of the person who assesses the classes for template information gathering.

V. EXPERIMENT RESULTS

We conducted both hardware testing and software testing. To characterize the fabricated analog PCB, we checked the gains and the cut-off frequencies by using artificial signals and tested the functionality of the spike detection circuitry by using a biological analog signal. We verified it independently from the digital PCB by using an I^2C-USB converter to communicate through a desktop computer. We tested the software module with raw data sets collected from dragonflies. In the preparations, the dragonfly's eyes were upside down to make recordings from the ventral nerve cord more conveniently. The stimulus screen (1440×900 $pixels$) was put next to the dragonfly. These recordings were implemented with a single hook electrode around the ventral nerve cord. The recorded signal was then stored in a digital format at a sampling rate of 50kHz.

A. PCB Validation

In the frequency response with switch settings of (BPF:$100Hz-5kHz$) the measured 3 dB points for the HPF and the LPF were 250 Hz and 3.8 kHz, respectively. Though the cut-off frequencies did not exactly match the theoretical settings, this fabricated PCB still meets the demands of the research. Fig. 2 shows a photo of the oscilloscope when we detected spikes from a biological signal with the circuit. The circuit detected spikes at very high speed, but because of the using very simple threshold algorithm it had a quite high false positive rate.

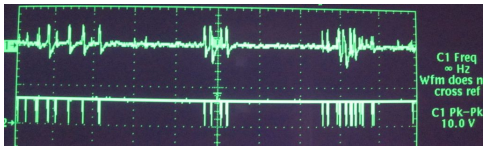

Fig. 2. Oscilloscope snapshot as verifying the spike detection circuit. The top is a raw input signal. The bottom presents the detected pulse output.

Immediately after power-up, the digital PCB consumed a low electric current (70 mA). After the soft-core processor was generated successfully, the configuration file was loaded to the FPGA. During the process of configuration, the electric current of the digital PCB was up to about 130 mA. When the process finished, the current returned to the initial value. We built a soft-core processor for the FPGA with the manufacturer's system integration tool. Using a host computer and the JTAG communication ("Joint Test Action Group" standard), we loaded these output files into the FPGA for the configuration step.

B. Spike-Sorting Application Tests

We gathered spike-pattern information for all six templates. Fig. 3 shows an example of the information we found to build the MDT4 template from spike patterns. The whole template set is shown in Fig. 4.We found that DIT1 and DIT3 had a similar amplitude range but they were different in the first half of their shapes. All the MDT group had a smaller amplitude range (just ± 1 V) than the DIT group had (± 3.2 V). To validate the whole template set, we tested again with new data sets that had similar settings to the ones we used to build templates, but were recorded in different preparations. During this period, we varied the correlation threshold level Cr and observed when we got unexpected template matching results. Figs. 5 and 6 show cases of testing for intended templates and the big arrows indicate a suggested Cr in the figures. We found $0.88 \rightarrow 0.9$ is the reasonable range of Cr for the template set.

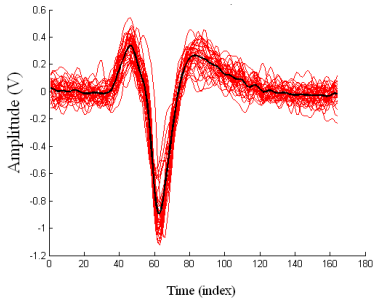

Fig. 3. The MDT4 template and the waveforms used to build it.

We sorted out spikes with different arbitrary settings of the stimulus. When the angle was small but not orthogonal to the axes of the screen (e.g. 48^o and 55^o), only DIT3s were indicated (Fig. 7). If the angle was also not orthogonal to the axes of the screen but closer to 90^o (e.g. 70^o), DIT1s

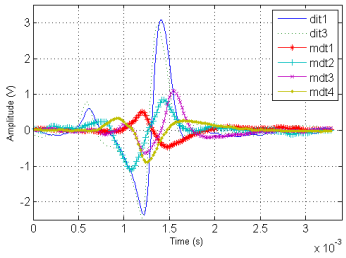

Fig. 4. The whole set of templates to compare their shapes.

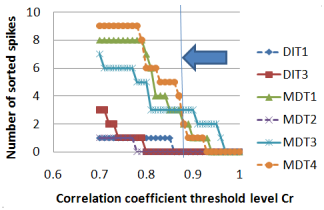

Fig. 5. Test case for MDT3, DIT3, and MDT1. MDT3 spikes dominate the observation among few DIT3 and MDT1 ones. Other TSDN spikes are considered unexpected results (dot line).

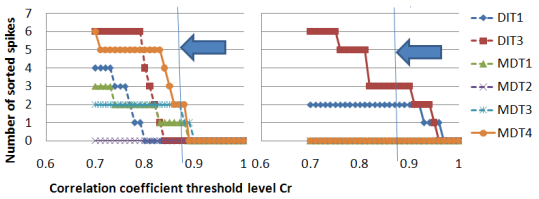

Fig. 6. Testing case for MDT4 (left) DIT3 and DIT1 (right). MDT4 spikes should dominate the left. DIT3 and DIT1 spikes should dominate the right. Other TSDN spikes are considered unexpected results (dot line).

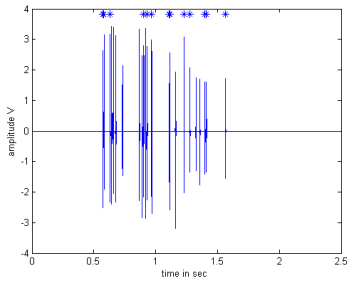

Fig. 7. Testing the template set with data set S201, 48^o from 700×0. When the angle was small but not orthogonal, only DIT3s were indicated (markers *) with a $Cr = 0.9$.

appeared but still less than DIT3. All of these observed results also agree with the investigation of visual receptive field properties by Frye et al. [7].

VI. CONCLUSION

Results confirmed that the template set agrees with the visual receptive field properties and can be used for spike sorting. The proposed system can work as a visual information processor in real time for dragonfly hybrid bio-robots. There are some limitations found in the fabricated PCBs. To fit a smaller robot platform, we should reduce PCB size by choosing new models of digital switches and potentiometers or finding a new method to vary the capacitance and resistance components. Currently, these ones cause a complicated I^2C communication network and a large space consumption. Though this system is aimed to dragonfly hybrid bio-robots, it can be modified for another kind of animal. Hence, the system may help better understand the representations and computational architectures used by different biological systems in neuroscience. Additionally, different spike-sorting algorithms can also be applied to the architecture. Consequently, the system can be used to evaluate recent spike-sorting algorithms with real neural signals instead of simulated ones.

REFERENCES

[1] K. Jeong, J. Kim, and L. P. Lee, "Biologically inspired artificial compound eyes," *Science, Materials and Biology*, vol. 310, pp. 557–560, 2005.

[2] L. P. Lee and R. Szema, "Inspirations from biological optics for advanced photonic systems," *Science, Materials and Biology*, vol. 310, pp. 1148–1150, 2005.

[3] L. I. Ortiz, "A mobile electrophysiology board for autonomous biorobotics," *MS thesis, Electrical and Computer Engineering Dept., University of Arizona*, December 2006.

[4] Z. Rivera-Alvidrez, "Computational modeling of neurons involved in fly motion detection," *MS thesis Electrical and Computer Engineering Dept., University of Arizona*, August 2005.

[5] T. Melano, "Insect-machine interfacing," *PhD thesis Biomedical Engineering, University of Arizona*, January 2011.

[6] R. M. Olberg, "Identified target-selective visual interneurons descending from the dragonfly brain," *Journal of Comparative Physiology A: Neuroethology, Sensory, Neural, and Behavioral Physiology*, vol. 159, pp. 827–840, 1986.

[7] M. A. Frye and R. M. Olberg, "Visual receptive field properties of feature detecting neurons in the dragonfly," *Comparative Physiology A: Neuroethology, Sensory, Neural, and Behavioral Physiology*, vol. 177, pp. 569–576, 1995.

[8] I. Obeid and P. Wolf, "Evaluation of spike-detection algorithms for a brain-machine interface application," *IEEE Transactions on Biomedical Engineering,*, pp. 905 –911, 2004.

[9] J. Kaiser, "On a simple algorithm to calculate the 'energy' of a signal," in *Acoustics, Speech, and Signal Processing, 1990. ICASSP-90., 1990 International Conference on*, vol. 1, 1990, pp. 381 –384.

[10] E. M. Glaser and W. B. Marks, "Separation of neuronal activity by waveform analysis," *Advances in Biomedical Engineering*, vol. 5, pp. 137–156, 1968.

[11] J. C. Letelier and P. P. Weber, "Spike sorting based on discrete wavelet transform coefficients," *Journal of Neuroscience Methods*, vol. 101, no. 2, pp. 93 – 106, 2000.

[12] S. Takahashi, Y. Anzai, and Y. Sakurai, "A new approach to spike sorting for multi-neuronal activities recorded with a tetrode–how ICA can be practical," *Neuroscience Research*, pp. 265 – 272, 2003.

[13] P. Cheeseman, J. Kelly, M. Self, J. Stutz, W. Taylor, and D. Freeman, "Autoclass: A Bayesian classification system," *Proc of the Fifth Intl Workshop on Machine Learning*, pp. 54–64, 1988.

[14] M. Blatt, S. Wiseman, and E. Domany, "Superparamagnetic clustering of data," *Phys. Rev. Lett.*, vol. 76, pp. 3251–3254, 1996.

[15] S. Gibson, J. W. Judy, and D. Markovic, "Comparison of spike-sorting algorithms for future hardware implementation," in *Engineering in Medicine and Biology Society, 2008.*, 2008, pp. 5015 –5020.

[16] S. Mukhopadhyay and G. Ray, "A new interpretation of nonlinear energy operator and its efficiency in spike detection," *IEEE Transactions on Biomedical Engineering*, vol. 45, pp. 180 –187, 1998.

[17] M. Blatt, S. Wiseman, and E. Domany, "Data clustering using a model granular magnet," *Neural Comput.*, vol. 9, pp. 1805–1842, 1997.